

Subharmonic resonance of a trapped wave near a vertical cylinder by narrow-banded random incident waves

Yile Li · Chiang C. Mei

Received: 6 February 2006 / Accepted: 31 October 2006 / Published online: 25 November 2006
© Springer Science+Business Media B.V. 2006

Abstract It is well-known that near an infinite linear array of periodically spaced cylinders trapped waves of certain eigenfrequencies can exist. If there are only a finite number of cylinders in an infinite sea, trapping is imperfect. Simple harmonic incident waves can excite a nearly trapped wave at one of the eigenfrequencies through a linear mechanism. However, the maximum amplification ratio increases monotonically with the number of the cylinders; hence the solution is singular in the limit of infinitely many cylinders. Recently, a nonlinear theory of subharmonic resonance of perfectly trapped waves has been completed. In this article the theory is further extended to random incident waves with a narrow spectrum centered near twice the natural frequency of the trapped wave. The effects of detuning and bandwidth of the spectrum are examined.

Keywords Landau–Stuart equation · Nonlinear resonance · Subharmonic resonance · Trapped wave

1 Introduction

Trapping of sinusoidal water waves, either by a stationary body in a channel or by an infinite and periodic array of bodies, has been extensively treated in the linearized framework by Evans and his associates in the past decade [1–7]. When trapping is perfect, these modes cannot be resonated by incident waves of the same frequency, according to the linearized theory. If there is only a finite number of periodically spaced cylinders in an infinite sea, then trapping is imperfect and synchronous resonance can be predicted by a linear theory [8].

Dedicated to Professor J. N. Newman on his 70th birthday. We wish to express our profound admiration for Professor Newman's scientific contributions and leadership in the ship-hydrodynamics discipline. The relation between this article and an early work of his reflects in part his impact on us.

Y. Li
Department of Mechanical Engineering, Massachusetts Institute of Technology, Cambridge, MA 02139, USA
e-mail: yl_li@mit.edu

C. C. Mei (✉)
Department of Civil and Environmental Engineering, Massachusetts Institute of Technology,
Cambridge, MA 02139, USA
e-mail: ccmei@mit.edu

In coastal oceanography it is known that perfectly trapped edge waves can also be present on a sloping beach of infinite length. Laboratory experiments by Galvin [9] have shown that an edge wave can be resonated nonlinearly by a sinusoidal incident wave of twice the edge-wave frequency. This observation has been explained by a nonlinear theory [10–13]. Of more recent interest in coastal engineering is the case of mobile barriers proposed for the inlets of Venice Lagoon for protecting the famed city from storm tides. Each of the four planned barriers is a series of 20 closely aligned hollow gates across an inlet. All gates are allowed to swing about a common axis on the seabed to reduce the forces on the supporting structure and the foundation, but are otherwise unattached to one another. It was, however, found in the laboratory that normally incident sea waves can force the neighboring gates to oscillate in opposite phases, at half the frequency. The cause for this undesirable oscillation was later found to be the existence of trapped modes owing to the periodic and mobile construction [14]. A nonlinear theory for monochromatic incident waves, similar to the subharmonic resonance of edge waves, has been given in [15], and confirmed by laboratory experiments. Chaotic response to deterministic narrow-banded incident waves was also found theoretically and verified by experiments [16]. For a somewhat more idealized barrier geometry and shallow water waves, Vittori [17] reported a stochastic theory for the excitation of gate oscillations by random incident waves with a narrow frequency band.

Recently we have completed a nonlinear theory for subharmonic resonance of monochromatic waves trapped by a vertical cylinder in a channel. The geometry is equivalent to one period in an infinite array of periodically spaced cylinders. The evolution equation for the amplitude of the trapped mode is found analytically to be a Landau–Stuart equation governing other trapped-wave resonance problems. The main task of calculating the coupling coefficients is achieved by solving a number of scattering or radiation problems. By numerical solution of these problems, the effects of the geometry on the resonance characteristics have been examined.

In this article we examine the response to random incident waves with a narrow frequency band. The spectrum is assumed to be Gaussian with prescribed bandwidth. The spectral peak is assumed to be slightly detuned from twice the eigenfrequency of the trapped mode. Because of the narrowness of the frequency band, the incident-wave amplitude is a slowly varying, though random, function of time. As a consequence, the amplitude of the trapped wave is also a slowly varying random function of time, governed by the Landau–Stuart equation which is of the same form as that for the deterministic problem. From many numerical solutions of the stochastic equation we shall examine statistically the averaged growth rate and averaged final amplitude as functions of detuning and spectral band width.

2 Summary of the deterministic theory

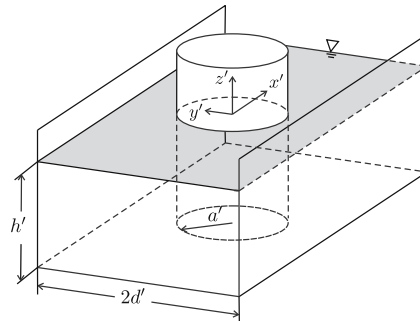
We consider a bottom-mounted circular cylinder of radius a' fixed at the center of a channel of width $2d'$ and depth h' . Let a Cartesian coordinate system be chosen such that the (x', y') -plane coincides with the still free surface and z' points upward along the cylinder axis, as shown in Fig. 1. A train of plane waves of amplitude A'_I arrives along the positive x' -axis and interacts with the cylinder.

For convenience we first outline the steps that lead to the evolution equation in the deterministic case.

Let the fluid be incompressible and inviscid, and the flow be irrotational. Denoting the ratio of the incident wave amplitude A'_I and the channel half-width¹ d' as $\epsilon^2 (= A'_I/d')$. It can be reasoned that the trapped-wave amplitude is of order $O(A'_I/\epsilon) = O(\sqrt{A'_I d'})$ if resonated by incident waves of amplitude A'_I . After normalization the free surface conditions are expanded in powers of ϵ to the third order. At the leading order only the trapped wave is present. The eigenfunction and the eigenfrequency are found by the hybrid finite-element method, where the solution is represented analytically by eigenfunction expansions

¹ The channel width $2d'$ can be thought of as the center-to center spacing of a periodic array of cylinders.

Fig. 1 Circular cylinder in a open channel



away from the cylinder but by discrete finite elements near the cylinder. At the second order, the scattered waves due to incoming waves of frequency $2\omega'_0$ are calculated. Due to quadratic interactions of the trapped wave with itself, there are radiated waves of frequency $2\omega'_0$ also. At the third order, cross-interaction between the first-order trapped waves and the second-order incident/scattered waves creates forcing which is oscillatory in time at the frequency ω'_0 . The condition for the solvability of the corresponding inhomogeneous boundary-value problem leads to the evolution equation for the complex amplitude B' of the trapped wave.

Let the following dimensionless variables be used,

$$t = \sqrt{\frac{g}{d'}}t', \quad (x, y, z, h) = \frac{(x', y', z', h')}{d'}, \quad k = k'd',$$

$$(\zeta, B) = \frac{(\zeta', B')}{\sqrt{A'_I d'}}, \quad A = \frac{A'_I}{\epsilon \sqrt{A'_I d'}} = 1, \quad \Phi = \frac{\Phi'}{d' \sqrt{g A'_I}}, \tag{2.1}$$

where ζ' denotes the free-surface displacement and B' is the amplitudes of the trapped wave. At the leading order the dimensionless potential of the trapped waves can be written as

$$\Phi = \frac{B}{2i\omega_0} \frac{\cosh k_0(z+h)}{\cosh k_0 h} \eta(x, y) e^{-i\omega_0 t} + \text{c.c.}, \tag{2.2}$$

where c.c. represents the complex conjugate of the preceding term. The dimensionless evolution equation for B is found to be the Landau–Stuart equation

$$-i \frac{dB}{d\tau} = c_\alpha B^2 B^* + c_\gamma A B^*, \tag{2.3}$$

where $\tau = \epsilon^2 t$ and $A = 1$. The coefficients are

$$c_\alpha = \frac{1}{E} \sum_{i=2}^9 \iint_{S_F} \alpha_i \Im(\eta) dS, \quad c_\gamma = \frac{1}{E} \sum_{i=2}^4 \iint_{S_F} \gamma_i \Im(\eta) dS, \tag{2.4}$$

where

$$E = \iint_{S_F} (\Im(\eta))^2 dS. \tag{2.5}$$

The coefficients $\alpha_i(x, y)$ and $\gamma_i(x, y)$ depend on the geometry and are discussed in detail in [18].

3 The stochastic problem

3.1 Random incident wave

For clarity we first describe the random incident waves in terms of physical variables distinguished by primes. Let the incident wave be a homogeneous, stationary random process, described by a Fourier–Stieltjes integral [19–21]

$$\zeta'(x', t') = \int_{-\infty}^{\infty} e^{i(k'x' - \omega't')} d\mathcal{A}'(\omega'), \tag{3.1}$$

where ω' is the frequency and k' is the wavenumber satisfying the dispersion relation

$$\omega'^2 = gk' \tanh k'h'. \tag{3.2}$$

Because of stationarity, the covariance between two random variables $d\mathcal{A}'(\omega')$ and $d\mathcal{A}'(\omega'_1)$ is

$$\langle d\mathcal{A}'(\omega') d\mathcal{A}'^*(\omega'_1) \rangle = \delta(\omega' - \omega'_1) S'(\omega') d\omega' d\omega'_1, \tag{3.3}$$

where the angle brackets denote the ensemble average. $S'(\omega')$ is the spectral density, which is real, non-negative and even, $S'(-\omega') = S'(\omega')$.

In (3.1), $d\mathcal{A}'(\omega')$ can be seen as the complex amplitude of the component wave of frequency between ω' and $\omega' + d\omega'$. The reality of ζ' implies the following symmetry

$$d\mathcal{A}'(-\omega') = d\mathcal{A}'^*(\omega'). \tag{3.4}$$

Thus, we can decompose (3.1) into two parts

$$\zeta'(x', t') = \int_0^{\infty} e^{i(k'x' - \omega't')} d\mathcal{A}'(\omega') + \int_{-\infty}^0 e^{i(k'x' - \omega't')} d\mathcal{A}'(\omega'), \tag{3.5}$$

where the second integral can be shown to be the complex conjugate of the first. The wave energy contained in the frequency range $0 < \omega' < \infty$ and $-\infty < \omega' < 0$ are equal. Hence half of the total energy is, by using (3.3)

$$\langle \zeta' \zeta'^* \rangle |_{\omega' > 0} = \int_0^{\infty} \int_0^{\infty} d\omega' d\omega'_1 \langle d\mathcal{A}'(\omega') d\mathcal{A}'(\omega'_1) \rangle = \int_0^{\infty} S'(\omega') d\omega' = \frac{1}{2} \int_{-\infty}^{\infty} S'(\omega') d\omega'. \tag{3.6}$$

and can be used to define the characteristic amplitude of the random incident wave

$$A'_I = \left(2 \int_{-\infty}^{\infty} S'(\omega') d\omega' \right)^{\frac{1}{2}}. \tag{3.7}$$

The small parameter ϵ is still defined in terms of the new A'_I by

$$\epsilon = \sqrt{\frac{A'_I}{d'}} \ll 1, \quad \text{or } \epsilon^2 = \frac{A'_I}{d'}. \tag{3.8}$$

Now we assume in addition that the incident-wave spectrum has a narrow bandwidth of order $O(\epsilon^2 \omega'_0)$. The spectral density $S'(\omega')$ peaks at $2\omega'_0 + \epsilon^2 2\Omega'$ and decays rapidly away from the peak. $2\epsilon^2 \Omega'$ is the detuning frequency. By the transformation

$$\omega' = \pm \left(2\omega'_0 + \epsilon^2 (2\Omega' + \sigma') \right), \quad \text{for } \omega' \geq 0, \tag{3.9}$$

we can change the argument of $d\mathcal{A}'$ from ω' to σ' . Accordingly, the free-surface displacement (3.5) becomes

$$\zeta'(x', t') = e^{-2i(\omega'_0 + \epsilon^2 \Omega')t'} \int_{-2\omega'_0/\epsilon^2 - 2\Omega'}^{\infty} e^{i(k'x' - \epsilon^2 \sigma't')} d\mathcal{A}'(\sigma') + \text{c.c.} \tag{3.10}$$

The lower limit of the integral in (3.10) is a large value of the order $O(\epsilon^{-2})$ and can be replaced by $-\infty$ in view of the assumption that the spectrum diminishes rapidly away from $2\omega'_0$. Note that the first integral in (3.10) includes only the contribution from the positive half of the two-sided spectrum S' . It follows from (3.3) and the identity $\delta(\lambda x) = \delta(x)/|\lambda|$, where λ is a constant, that the covariance of $d\mathcal{A}'(\sigma')$ obeys

$$\langle d\mathcal{A}'(\sigma') d\mathcal{A}'^*(\sigma'_1) \rangle = \epsilon^2 \delta(\sigma' - \sigma'_1) \tilde{S}'(\sigma') d\sigma' d\sigma'_1. \tag{3.11}$$

where

$$\tilde{S}'(\sigma') = \begin{cases} S'(2\omega'_0 + \epsilon^2(2\Omega' + \sigma')), & \sigma' > -2\omega'_0/\epsilon^2 - 2\Omega', \\ 0, & \text{otherwise,} \end{cases} \tag{3.12}$$

takes non-zero values only in the positive half of the frequency range of ω' .

Consequently, Eq. (3.6) becomes

$$\langle \zeta' \zeta'^* \rangle |_{\omega' > 0} = \int_{-\infty}^{\infty} \int_{-\infty}^{\infty} d\sigma' d\sigma'_1 \langle d_{\mathcal{A}'}(\sigma') d_{\mathcal{A}'}(\sigma'_1) \rangle = \epsilon^2 \int_{-\infty}^{\infty} \tilde{S}'(\sigma') d\sigma' = \frac{1}{2} \int_{-\infty}^{\infty} S'(\omega') d\omega', \tag{3.13}$$

which indicates that the incident-wave energy is of the order of $O(\epsilon^2)$ and hence small.

3.2 Normalized incident waves

Using A'_I defined in (3.7) as the scale of the incident wave, we introduce the following normalized variables in addition

$$(\omega, \Omega, \omega_o, \sigma) = \sqrt{\frac{d'}{g}} (\omega', \Omega', \omega'_o, \sigma'), \quad k = k' d',$$

$$d_{\mathcal{A}} = \frac{2d_{\mathcal{A}'}}{A'_I}, \quad \tilde{S} = \frac{4g^{\frac{1}{2}}}{A'_I d'^{\frac{3}{2}}} \tilde{S}'.$$

The purpose of using the factors 2 and 4 in the scales of $d_{\mathcal{A}'}$ and \tilde{S}' , respectively, will become clear shortly.

In dimensionless variables, the free-surface displacement (3.10) becomes,

$$\zeta(x, t) = \frac{\epsilon}{2} e^{-2i\omega_0 t} e^{-2i\Omega \tau} \int_{-\infty}^{\infty} e^{i(kx - \sigma \tau)} d_{\mathcal{A}}(\sigma) + \text{c.c.} + O(\epsilon^4), \tag{3.14}$$

where $\tau = \epsilon^2 t$ is the slow time variable. The wavenumber k is related to ω by the dimensionless form of the dispersion relation (3.2)

$$k \tanh kh = \omega^2. \tag{3.15}$$

Letting

$$k = K + \epsilon^2 K_2 + O(\epsilon^4), \tag{3.16}$$

we can easily find from (3.9) and (3.15) that

$$K \tanh Kh = 4\omega_0^2, \quad K_2 = \frac{4\omega(\sigma + 2\Omega)}{\tanh Kh + Kh(1 - \tanh^2 Kh)}. \tag{3.17}$$

Therefore by substituting (3.16) in (3.14), we get, up to the second order

$$\zeta(x, t) = \frac{\epsilon}{2} \left\{ e^{-2i\Omega \tau} \int_{-\infty}^{\infty} e^{i(K_2 x_2 - \sigma \tau)} d_{\mathcal{A}}(\sigma) \right\} e^{i(Kx - 2\omega_0 t)} + \text{c.c.}, \tag{3.18}$$

with $x_2 = \epsilon^2 x$ the slow spatial coordinate. Near the cylinder, we set $x_2 = 0$. Moreover, let us introduce

$$A(\tau) = e^{-2i\Omega \tau} \int_{-\infty}^{\infty} e^{-i\sigma \tau} d_{\mathcal{A}}(\sigma) = \hat{A} e^{-2i\Omega \tau}, \quad \text{where} \quad \hat{A} = \int_{-\infty}^{\infty} e^{-i\sigma \tau} d_{\mathcal{A}}(\sigma), \tag{3.19}$$

as the wave envelope amplitude is varying stochastically with respect to the slow time τ . Accordingly, we express the random incident wave in the simple form

$$\zeta(x, t) = \frac{\epsilon}{2} A(\tau) e^{i(Kx - 2\omega_0 t)} + \text{c.c.}, \tag{3.20}$$

The random amplitude $A(\tau)$ must be determined from the incident-wave spectrum. From (3.11), the covariance of the dimensionless increment $d\mathcal{A}(\sigma)$ is now given by

$$\langle d\mathcal{A}(\sigma)d\mathcal{A}^*(\sigma_1) \rangle = \delta(\sigma - \sigma_1)\tilde{S}(\sigma)d\sigma d\sigma_1, \quad (3.21)$$

where, from (3.13), one can show that the spectral-density function $\tilde{S}(\sigma)$ satisfies the normalizing condition,

$$\int_{-\infty}^{\infty} \tilde{S}(\sigma) d\sigma = 1. \quad (3.22)$$

The forms of (3.14), (3.21) and (3.22) are the result of introducing the factors 2 and 4 in the normalization of \mathcal{A}' and \tilde{S}' , respectively. To evaluate the complex amplitude $A(\tau)$ numerically, we rewrite (3.19) as

$$A(\tau) = e^{-2i\Omega\tau} \sum_{m=-\infty}^{\infty} |d\mathcal{A}(\sigma_m)| e^{-i\sigma_m\tau - i\arg[d\mathcal{A}(\sigma_m)]}. \quad (3.23)$$

The prescribed spectrum \tilde{S} is discretized into vertical strips of width $\Delta\sigma$ and height $\tilde{S}(m\Delta\sigma)$. The frequency of the m -th wave component σ_m is chosen randomly between $(m-1/2)\Delta\sigma$ and $(m+1/2)\Delta\sigma$. The amplitude is then calculated from

$$|d\mathcal{A}(\sigma_m)| = \tilde{S}^{1/2}(\sigma_m) \Delta\sigma, \quad (3.24)$$

while the phase angle $\arg[d\mathcal{A}(\sigma_m)]$ is chosen randomly according to a probability distribution uniform in $[0, 2\pi]$. More details can be found in [22, Chap. 2].

In the present study, we assume that the spectral function $\tilde{S}(\sigma)$ is Gaussian with zero mean and variance D^2 :

$$\tilde{S}(\sigma) = \frac{1}{\sqrt{2\pi}D} \exp\left(-\frac{\sigma^2}{2D^2}\right), \quad (3.25)$$

which depends only on the standard deviation D .

3.3 Stochastic evolution equation of trapped wave

For each realization, the trapped-wave amplitude is still given by (2.3), except that now the wave amplitude is given by (3.19). With the transformation

$$B = \hat{B}e^{-i\Omega\tau}, \quad (3.26)$$

Eq. 2.3 becomes

$$-i\frac{d\hat{B}}{d\tau} = c_\alpha \hat{B}^2 \hat{B}^* + \Omega \hat{B} + c_\gamma \hat{A}(\tau) \hat{B}^*. \quad (3.27)$$

which is a stochastic differential equation. For the deterministic Landau–Stuart equation (2.3), the equilibrium states and their linearized instability have been studied by [13] for edge waves. We now focus attention on the statistical analysis.

4 Nonlinear resonance excited by random waves

For the complete development of the trapped-wave amplitude we must solve the non-autonomous stochastic Landau–Stuart equation (2.3) numerically with a random complex coefficient $c_\gamma A(\tau)$. From (3.26), the magnitude $|B|$ is the same as $|\hat{B}|$ solved from (2.3). The statistical characteristics of the trapped-wave amplitude $|B|$ are determined from a large number of realizations with the phase angles in (3.19)

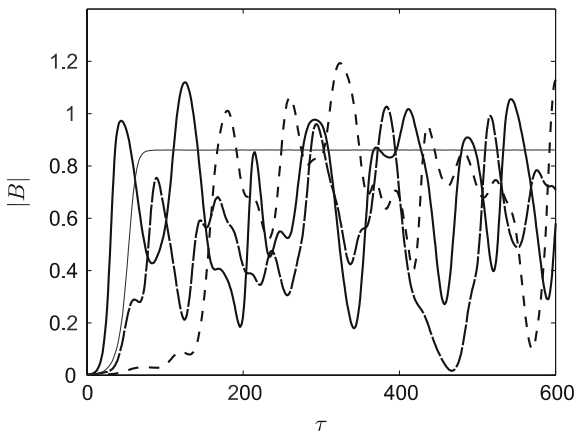


Fig. 2 Samples of trapped-wave amplitude $|B(\tau)|$ for different sets of phase angles, $a = 0.5, h = 1.0$. The coefficients $c_\alpha = -0.0135 + 0.1543i, c_\gamma = 0.0769 + 0.0851i, D/|c_\gamma| = 0.5, \Omega = 0.0$. Thin solid line: solution of deterministic incident wave

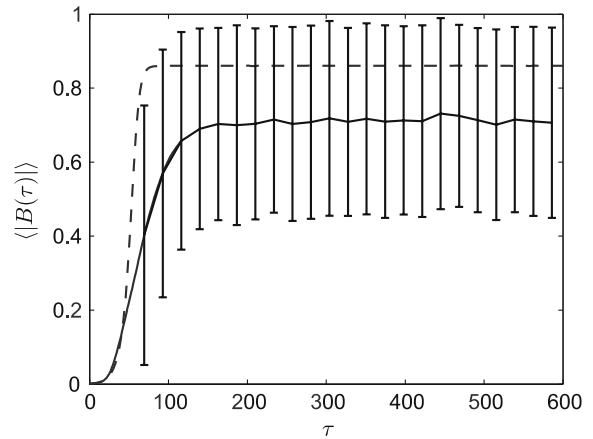


Fig. 3 Ensemble average and standard deviation of $|B(\tau)|$ compared with deterministic solution. Solid curve: $\langle |B| \rangle$, error bar: $\pm(\sigma)_B$, dashed curve: $|B|$ for deterministic incident wave

randomly generated from a uniform distribution between 0 and 2π and the initial value of $|B|$ at $\tau = 0$ randomly assigned with some small values less than 10^{-4} .

In Fig. 2, we display three nonlinear solutions of the Landau–Stuart equation (2.3), and compare them with the deterministic solution. Starting from an infinitesimal disturbance, the trapped-wave amplitude $|B|$ grows initially at a rate depending on the randomly assigned phase angle, and becomes a stationary random process thereafter.

The observed trapped-wave amplitude $|B|$ at an arbitrary instant τ is a random variable. Let us define the ensemble average of the trapped-wave amplitude at time τ by

$$\langle |B(\tau)| \rangle = \frac{1}{N} \sum_{n=1}^N |B_n(\tau)|, \tag{4.1}$$

and the standard deviation

$$\langle \sigma \rangle_B = \left[\frac{1}{N} \sum_{n=1}^N \left(|B(\tau)|_n - \langle |B(\tau)| \rangle \right)^2 \right]^{\frac{1}{2}}. \tag{4.2}$$

where n is the index of a realization and N the total number of realizations. In Fig. 3, the time development of the ensemble average and standard variance of $|B|$ are plotted. A total of 2048 realizations of $|B|$ with different phase angles are computed. It can be seen that the ensemble average increases from an infinitesimal disturbance and approaches a constant when τ is large, so is the variance. In comparison with the deterministic forcing represented by the dashed line in Fig. 3, the ensemble average grows more slowly and reaches a lower equilibrium value. These results are similar to [17] for Venice gates.

In [18], it is shown for a deterministic incident wave that the bifurcation curve representing the variation of equilibrium action versus detuning frequency can lean either to the right or to the left, depending on the sign of c_α . Hysteresis (jump phenomenon) can occur. Figs. 4 and 5 show the equilibrium values of the ensemble average $\langle |B| \rangle$ and the standard variance $\langle \sigma \rangle_B$ for various narrowband width D when $a = 0.30, h = 0.50$. The real part $\Re(c_\alpha) = -0.772$ is negative and the bifurcation curve leans rightward.² It can be

² In [18] the ordinates of the bifurcation curves were $|B|^2$ instead of $\langle |B| \rangle$, hence appear slightly different.

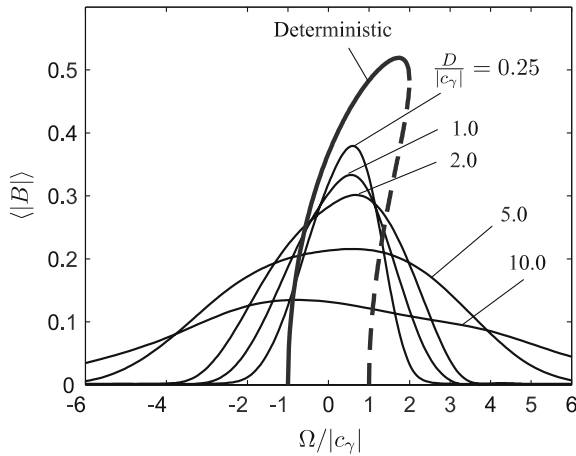


Fig. 4 Dependence of the ensemble average of the trapped-wave amplitude on D and Ω , $a = 0.30$, $h = 0.50$. The coefficients $c_\alpha = -0.772 + 0.4466i$, $c_\gamma = -0.0066 + 0.1202i$. The thick curve is for the deterministic incident wave and the thin curves are for random waves of various $D/|c_\gamma|$

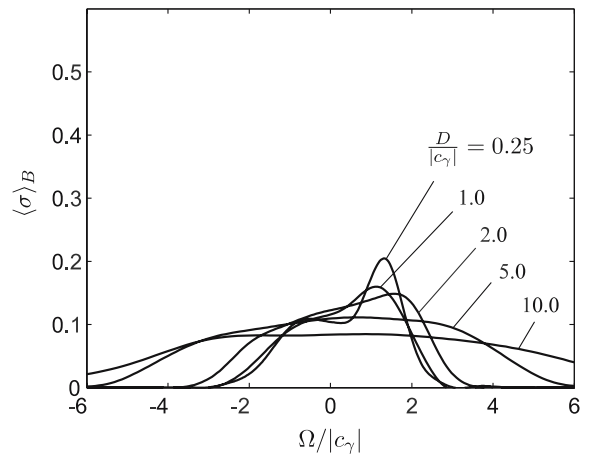


Fig. 5 Dependence of the ensemble standard variance of the trapped-wave amplitude on D and Ω , $a = 0.30$, $h = 0.50$. The coefficients $c_\alpha = -0.772 + 0.4466i$, $c_\gamma = -0.0066 + 0.1202i$

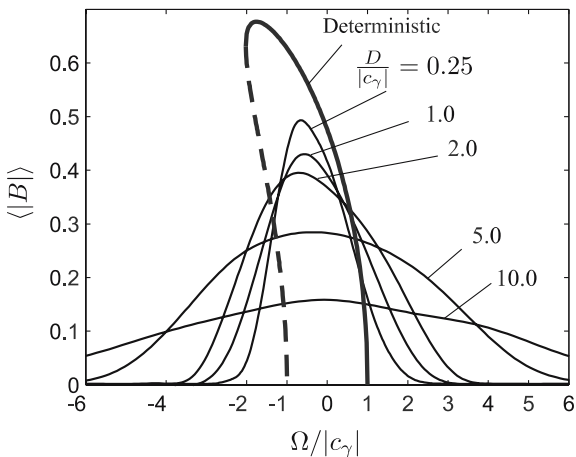


Fig. 6 Dependence of the ensemble average of the trapped-wave amplitude on D and Ω , $a = 0.32$, $h = 1.50$. The coefficients $c_\alpha = 0.4911 + 0.2794i$, $c_\gamma = 0.1265 + 0.020i$. The thick curve is for the deterministic incident wave and the thin curves are for random waves of various $D/|c_\gamma|$

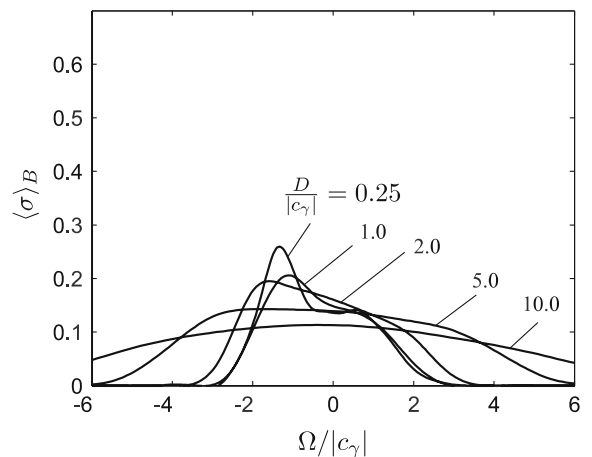


Fig. 7 Dependence of the ensemble standard variance of the trapped-wave amplitude on D and Ω , $a = 0.32$, $h = 1.50$. The coefficients $c_\alpha = 0.4911 + 0.2794i$, $c_\gamma = 0.1265 + 0.020i$

seen that, as the width D of the incident wave spectrum increases, the bifurcation curve becomes flatter and the trapped wave can be excited within a wider range of Ω , but to a smaller amplitude. Both bifurcation curves of $\langle |B| \rangle$ and $\langle \sigma \rangle_B$ of the randomly resonated trapped wave share the same sense of leaning as the deterministic case. However, there is no jump phenomenon in all the random cases calculated with $D > 0$. Figures 6 and 7 show the results for $a = 0.32$ and $h = 1.50$ where $\Re(c_\alpha) = 0.4911$ is positive and the bifurcation curves lean leftward. Again there is no hysteresis, and the amplification diminishes with D .

5 Concluding remarks

This work is an extension of our recent theory on nonlinear subharmonic resonance of perfectly trapped waves around a vertical cylinder in a long channel ([18]). A trapped mode of natural frequency ω and magnitude of $O(\epsilon)$ is excited by a much weaker $O(\epsilon^2)$ incident wave of frequency near 2ω . The extension here is to allow the incident wave to be random with a narrow frequency spectrum centered around 2ω , as in [17] on the mobile storm barrier of Venice. We have shown that the subharmonic resonance mechanism can still be effective. However, if the bandwidth is large enough, the amplification ratio is small; therefore the subharmonic mechanism becomes ineffective. Other extensions are possible. For example, one can treat a train of deterministic incident waves of magnitude comparable to the trapped wave, i.e., $O(\epsilon)$ and of frequency ω . Quadratic interaction then produces a $O(\epsilon^2)$ wave of 2ω which can resonate the trapped mode at $O(\epsilon^3)$ through the same subharmonic mechanism. Although the frequencies of the forcing and the response are the same, this mechanism is strictly nonlinear and leads to finite amplification. More generally, one may have two $O(\epsilon)$ deterministic incident waves of frequencies ω_1 and ω_2 . As long as $\omega_1 + \omega_2 \approx 2\omega$, similar nonlinear resonance can occur. In nature, the total wave energy is distributed over a broad band of frequencies. Then quadratic interactions of waves from different pairs in the broad spectrum may all contribute to the resonance of a trapped wave. It would be worthwhile to examine further the effects of random incident waves with a broad bandwidth. Finally, trapped waves of other types such as edge waves on a beach and trapped modes along the mobile barrier of Venice are likely subjected to similar excitations.

The mathematical problem studied here is equivalent to that for an infinitely long array of periodically spaced cylinders under attack by a train of normally incident plane waves. In the existing linear theory of a related problem studied by Professor Newman and Dr Maniar [8], synchronous resonance is possible only if the number of cylinders in an infinite sea is finite so that trapping is imperfect due to radiation damping. The linear theory ultimately fails in the limit of infinitely many cylinders as the resonant amplitude becomes unbounded. We therefore hope that the present work provides a complementary view to render a more complete picture of a fascinating subject.

Acknowledgements We acknowledge with gratitude the financial support by U.S. Office of Naval Research (Grant N00014-04-1-0077), US National Science Foundation (Grant CTS 0075713) and US-Israel BiNational Science Foundation (Grant 2004205).

References

1. Evans DV, Linton CM (1991) Trapped modes in open channels. *J Fluid Mech.* 225:153–175
2. Callan M, Linton CM, Evans DV (1991) Trapped modes in two-dimensional waveguides. *J Fluid Mech* 229:51–64
3. Linton CM, Evans DV (1992) Integral equations for a class of problems concerning obstacles in waveguides. *J Fluid Mech* 245:349–365
4. Evans DV, Levitin M, Vassiliev D (1994) Existence theorems for trapped modes. *J Fluid Mech* 261:21–31
5. Evans DV, Porter R (1997) Trapped modes about multiple cylinders in a channel. *J Fluid Mech* 339:331–356
6. Evans DV, Porter R (1998) Trapped modes embedded in the continuous spectrum. *Q J Mech Appl Maths* 52:263–274
7. Utsunomiya T, Taylor RE (1999) Trapped modes around a row of circular cylinders in a channel. *J Fluid Mech* 386:259–279
8. Maniar HD, Newman JN (1997) Wave diffraction by a long array of cylinders. *J. Fluid Mech* 339:309–330
9. Galvin CJ (1965) Resonant edge waves on laboratory beaches. *EOS Trans.* 46:112
10. Guza RT, Davis RE (1974) Excitation of edge waves by waves incident on a beach. *J Geophys Res* 79:1285–1291
11. Guza RT, Bowen AJ (1976) Finite amplitude Stokes edge waves. *J Marine Res* 34:269–293
12. Minzoni AA, Whitham GB (1977) On the excitation of edge wave on beaches. *J Fluid Mech* 79:273–287
13. Rockliff N (1978) Finite amplitude effects in free and forced edge waves. *Math Proc Cambridge Philos Soc* 83:463–479
14. Mei CC, Sammarco P, Chan ES, Procaccini C (1994) Subharmonic resonance of proposed storm Venice gates for Venice Lagoon. *Proc R Soc London A* 444:257–265
15. Sammarco P, Tran HH, Mei CC (1997a) Subharmonic resonance of Venice gates in waves. Part 1. Evolution equation and uniform incident waves. *J Fluid Mech* 349:295–325
16. Sammarco P, Tran HH, Gottlieb O, Mei CC (1997b) Subharmonic resonance of Venice gates in waves. Part 2. Sinusoidally modulated incident waves. *J Fluid Mech* 349:327–359

17. Vittori G (1998) Oscillating tidal barriers and random waves. *J Hydraulic Engng* 124:406–412
18. Li Y, Mei CC (2006) Subharmonic resonance of a trapped wave near a vertical cylinder in a channel. *J Fluid Mech* 561:391–416
19. Phillips O (1966) *The dynamics of the upper ocean*. Cambridge university press
20. Kinsman B (1984) *Wind waves: their generation and propagation on the ocean surface*. Dover, pp 330–331
21. Sveshnikov AA (1966) *Applied methods of the theory of random functions*. Pergamon press
22. Goda Y (2000) *Random seas and design of maritime structures*, 2nd edn. World Scientific, Singapore